## SUPPLEMENTARY MATERIALS

## Methods

Two lines of geologic research were conducted in order to investigate the role of hydrated minerals in VM landslide transport: (1) systematic mapping of landslide morphology and their relationships to nearby features, and (2) correlation of landslide morphology to their mineralogical compositions. The first task was completed based on analysis of THEMIS, CTX, and HiRISE imagery data; the second by analyzing CRISM near-infrared spectral data from the same landslide systems documented by photogeologic investigations.

### *Satellite Image Data and Methods*

Satellite images of Mars are available publicly via web access at http://www-pdsimage.jpl.nasa.gov/PDS/public/. Spatial resolutions of images analyzed are as following: (1) ~18 m/pixel for THEMIS images (Christensen et al., 2004), (2) ~5.2 m/pixel for CTX images (Malin et al., 2007), and (3) ~30 cm/pixel for HiRISE images (McEwen et al., 2007). Following the procedure of Schultz et al. (2010) and Yin (2012a,b), we conducted systematic mapping of landslides and their spatial relations with surrounding rocks directly on satellite images.

Landslide transport is fundamentally governed by Amonton's law for frictional properties of rocks:

$$\tau_n/\sigma_n = \mu \quad (1)$$

where $\tau_n$ is shear stress during sliding, $\mu$ is the coefficient of friction, and $\sigma_n$ is normal stress on the sliding plane. In order to estimate the normal stress initially exerted at the base of the landslide, we assume: (1) a maximum density of 2500 kg/m$^3$ (i.e., for fractured basalt) for the

landslide material (e.g., Hungr and Evans, 2004), (2) a maximum landslide thickness of 1800 m, and (3) a surface gravitational acceleration of 3.71 $m/s^2$.

***CRISM Data and Methods***

Composition of exposed rocks was determined using the CRISM hyperspectral imaging spectrometer, which takes targeted observations in 544 6.55-nm-wide channels in the visible to near-infrared (VNIR) (Murchie et al., 2007). "L" detector TRDR observations in the 1.0-4.0 μm wavelengths were analyzed to identify the presence of hydrated minerals. Water in minerals is characterized by vibrational absorptions between 1.91 and 1.95 μm from $H_2O$ and between 1.40 and 1.45 μm induced by OH and $H_2O$ (Clark et al., 1990).

In the regional survey of VM long-runout landslides (Fig. 1A), CRISM images examined include FRT0000B939 (see **Fig. 1B**), FRT000093E3, HRL0000A8F6, HRL0000A432, and HRL0000508A (clays detected- blue circles in **Fig. 1A**), as well as FRT0001672B, FRT0000B510, FRT0001892B and FRT000195E8, FRT00009D64 and HRL00019803, and HRL00019505 (no detectable hydrated minerals- red circles in **Fig. 1A**). For the landslide studied in detail (**Fig. 1B**), CRISM images analyzed include FRT0000BDF1 (CM-1), FRT0000D243 and FRT0001883A (overlapping CM-2 and CM-3), FRT0000A834 (CM-4), and HRL00007AA5 (CM-5) (no detectable hydrated minerals- orange boxes in Fig. 1B), as well as FRT0000B939 (CM-6) (with hydrated minerals- blue box in **Fig. 1B**; also see **Figs. 2A and 2E**).

Using the CRISM Analysis Toolkit (CAT) produced by the CRISM Science Team, the standard CRISM photometric and atmospheric corrections were applied to each image by dividing each pixel by the cosine of the incidence angle and by a scaled atmospheric transmission spectrum derived from observations of Olympus Mons (e.g. Roach et al., 2010).

Spectral summary parameters were calculated from diagnostic absorptions to facilitate preliminary identification and mapping of distinct geologic regions within a CRISM image (e.g. Pelkey et al., 2007). Summary parameters used in this study include the 1.9 μm band depth, due to combinations of $H_2O$ bending and stretching vibrations (BD1900); the 2.21–2.27 μm band depth (BD2200), and the 2.3 μm band depth (D2300), both due to metal-OH vibrations (e.g. Roach et al., 2010).

Spectra over areas of interest were generated by averaging signals in an area of 7x7 pixels. The signals were then normalized by dividing the spectra of interest by the spectrum of a spectrally neutral or unremarkable region (usually corresponding to Mars dust) in the same detector column. This procedure highlights spectral differences among areas of different geologic units and removes residual atmospheric and instrument artifacts (e.g. Roach et al., 2010). These ratioed spectra were visually compared to RELAB and USGS library laboratory reflectance spectra within the wavelengths of CRISM data for potential matches in diagnostic absorption band location and depth, and spectral shape. Map-projected composition data were integrated in a GIS framework with geologic maps created by interpreting CTX and HiRISE orbital imagery.

| **CRISM image ID** | **Interpreted spectral unit** | **Representative ROI center pixel** | |
|---|---|---|---|
| | | Numerator | Denominator |
| FRT0000B939 | Hydrated “doublet” (CM-6) | X: 321 Y: 201 | X: 324 Y: 17 |
| | Hydrated smectite (CM-6) | X: 328 Y: 277 | X: 324 Y: 17 |
| HRL0000A8F6 | Hydrated “doublet” | X: 270 Y: 200 | X: 288 Y: 46 |
| | Hydrated smectite | X: 144 Y: 274 | X: 143 Y: 146 |
| HRL00007AA5 | Unhydrated inner zone (CM-5) | X: 136 Y: 192 | X: 123 Y: 376 |

Supplementary Table 1. List of CRISM data subset for which spectra are presented in the text. Pixel locations of regions of interest (ROI) from which representative unit spectra were taken are provided.

**Supplementary References**

Clark, R. N., Gallagher, A. J., & Swayze, G. A., 1990, Material absorption band depth mapping of imaging spectrometer data using a complete band shape least-squares fit with library reference spectra: In Proceedings of the Second Airborne Visible/Infrared Imaging Spectrometer (AVIRIS) Workshop, v. 2, p. 4-5.

Pelkey, S.M., et al., 2007, CRISM multispectral summary products: Parameterizing mineral diversity on Mars from reflectance: Journal of Geophysical Research, v. 112, no. E8, doi:10.1029 /2006JE002831.

Schultz, R. A., Hauber, E., Kattenhorn, S. A., Okubo, C. H., & Watters, T. R., 2010, Interpretation and analysis of planetary structures: Journal of Structural Geology, v. 32, p. 855-875.

Yin, A., 2012a, Structural analysis of the Valles Marineris fault zone: Possible evidence for large-scale strike-slip faulting on Mars: Lithosphere, v. 4, p. 286-330.

Yin, A., 2012b, An episodic slab-rollback model for the origin of the Tharsis rise on Mars: Implications for initiation of local plate subduction and final unification of a kinematically linked global plate-tectonic network on Earth: Lithosphere, v. 4.6, p. 553-593.

**Supplementary Figures**

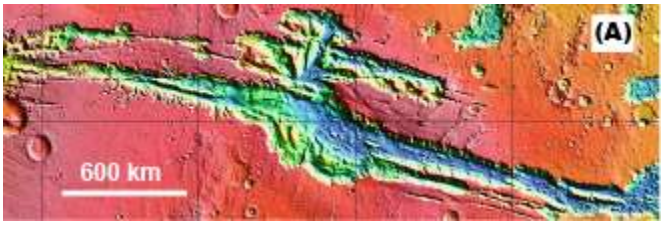


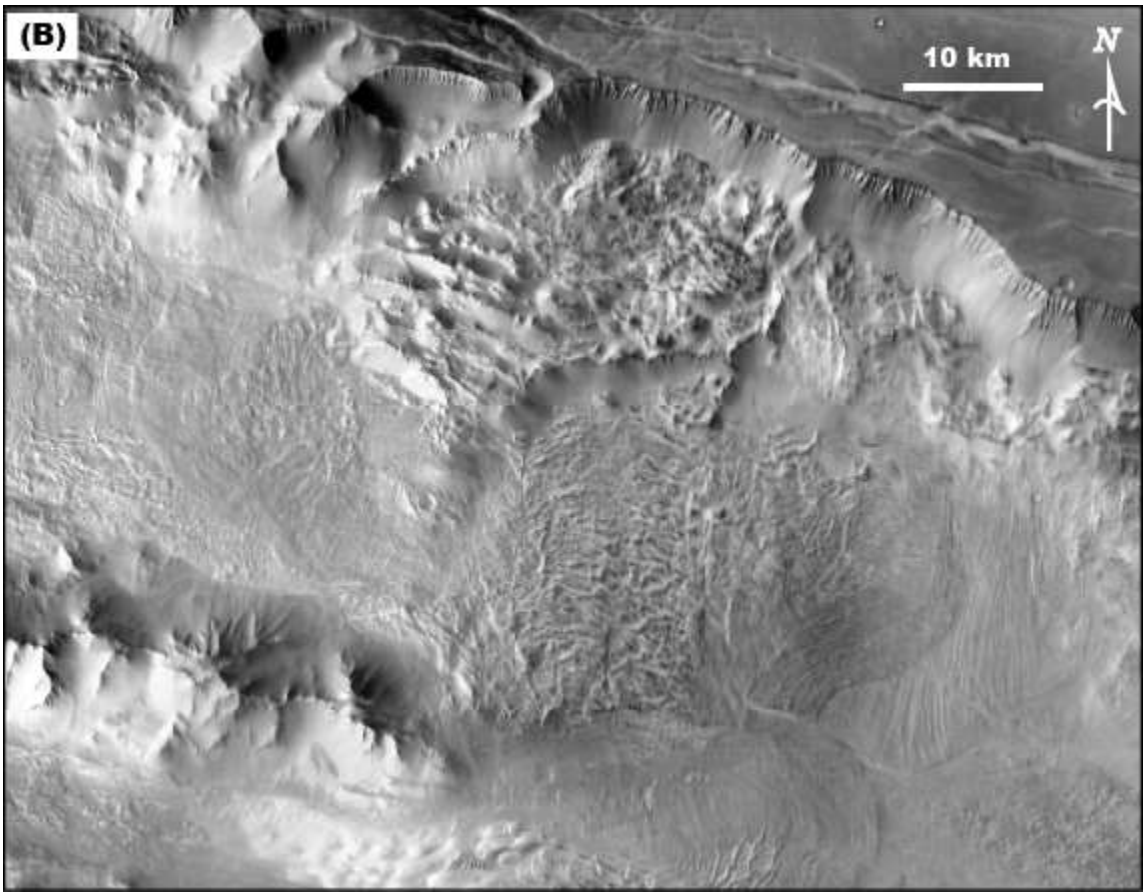


Supplementary Figure 1. (A) Unmarked image in **Fig. 1A**. (B) Unmarked THEMIS mosaic in **Fig. 1B**.

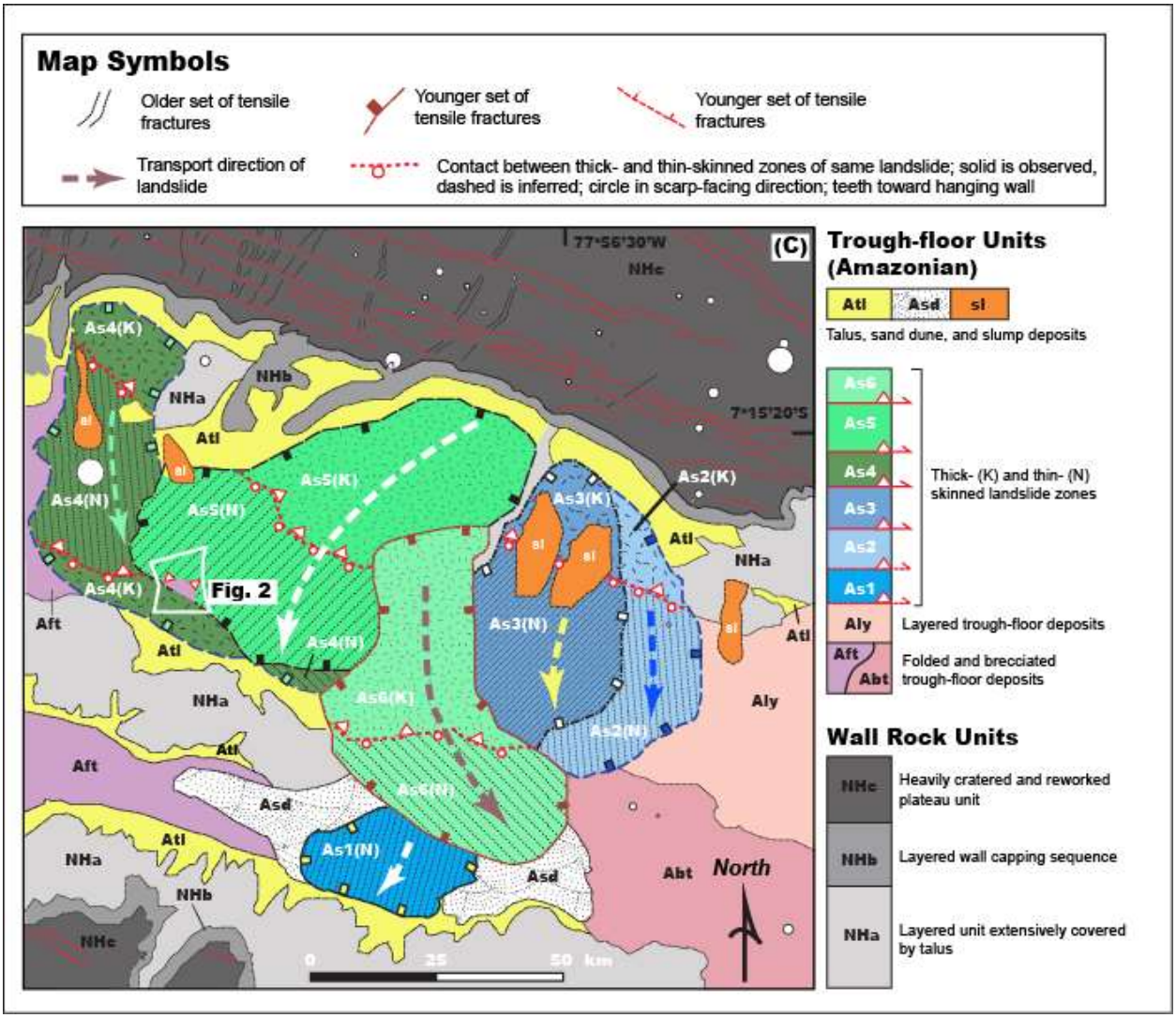


(C) Detailed geologic context map of the Ius Chasma study area and locations of the satellite and CRISM images in **Fig. 2**. Landslide transport direction inferred from lobe shape of the deposit. Amazonian talus, sand dune, and slump deposits postdate landslide emplacement; all wall rock is Noachian-Hesperian in age. NHa is exposed as scarps of landslide breakaways and linear scarps against the trough floor, NHb is the layered wall capping unit on top of the trough wall, and NHc contains crater ejecta, fluvial sediment, dust and aeolian deposits. Landslide As5 is the focus of this work, and is one of several lobes comprising a single landslide complex.

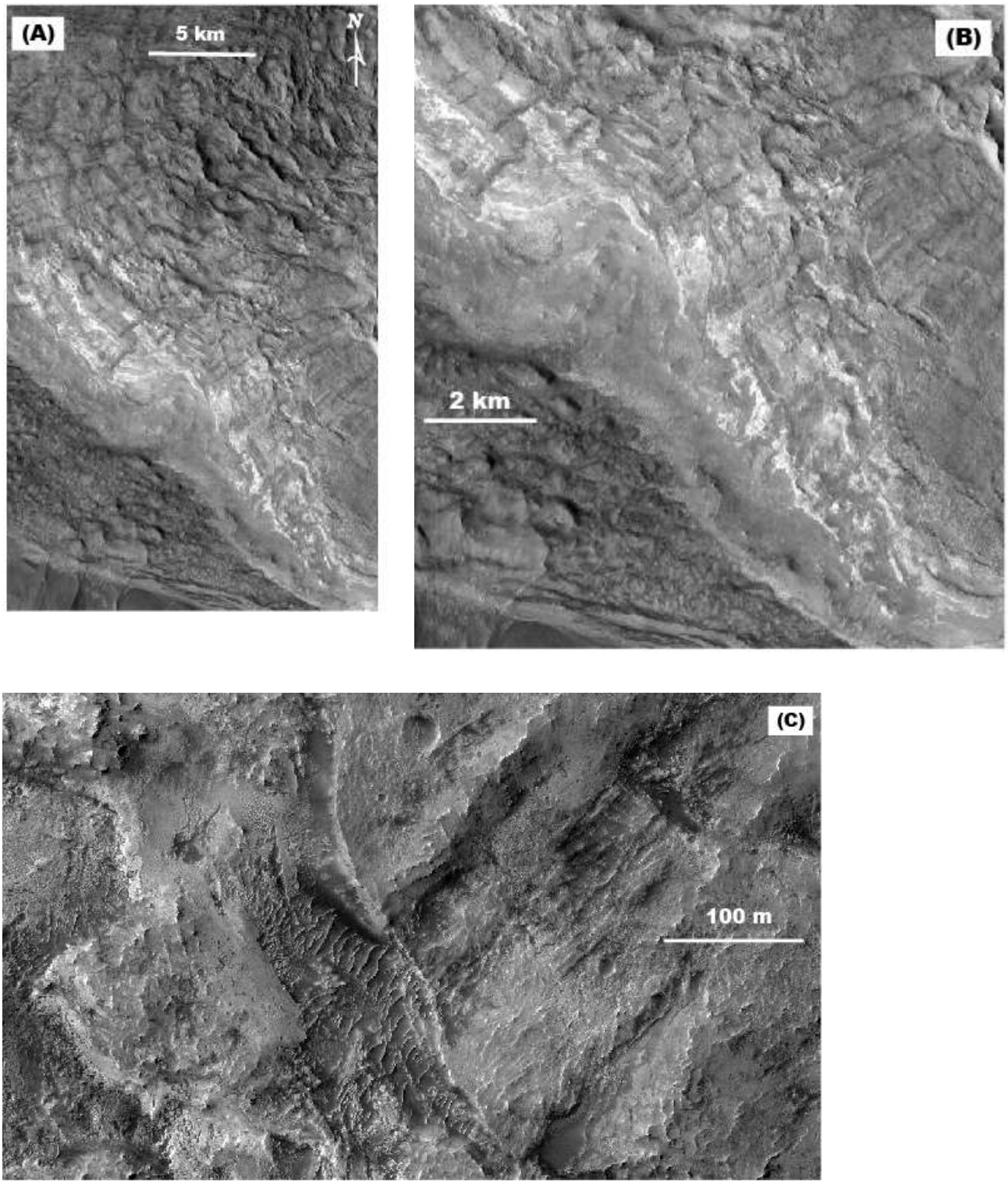


Supplementary Figure 2. (A) Unmarked CTX image in **Fig. 2B**. (B) Unmarked CTX image in **Fig. 2B**. (C) Unmarked HiRISE image in **Fig. 2C**.

D

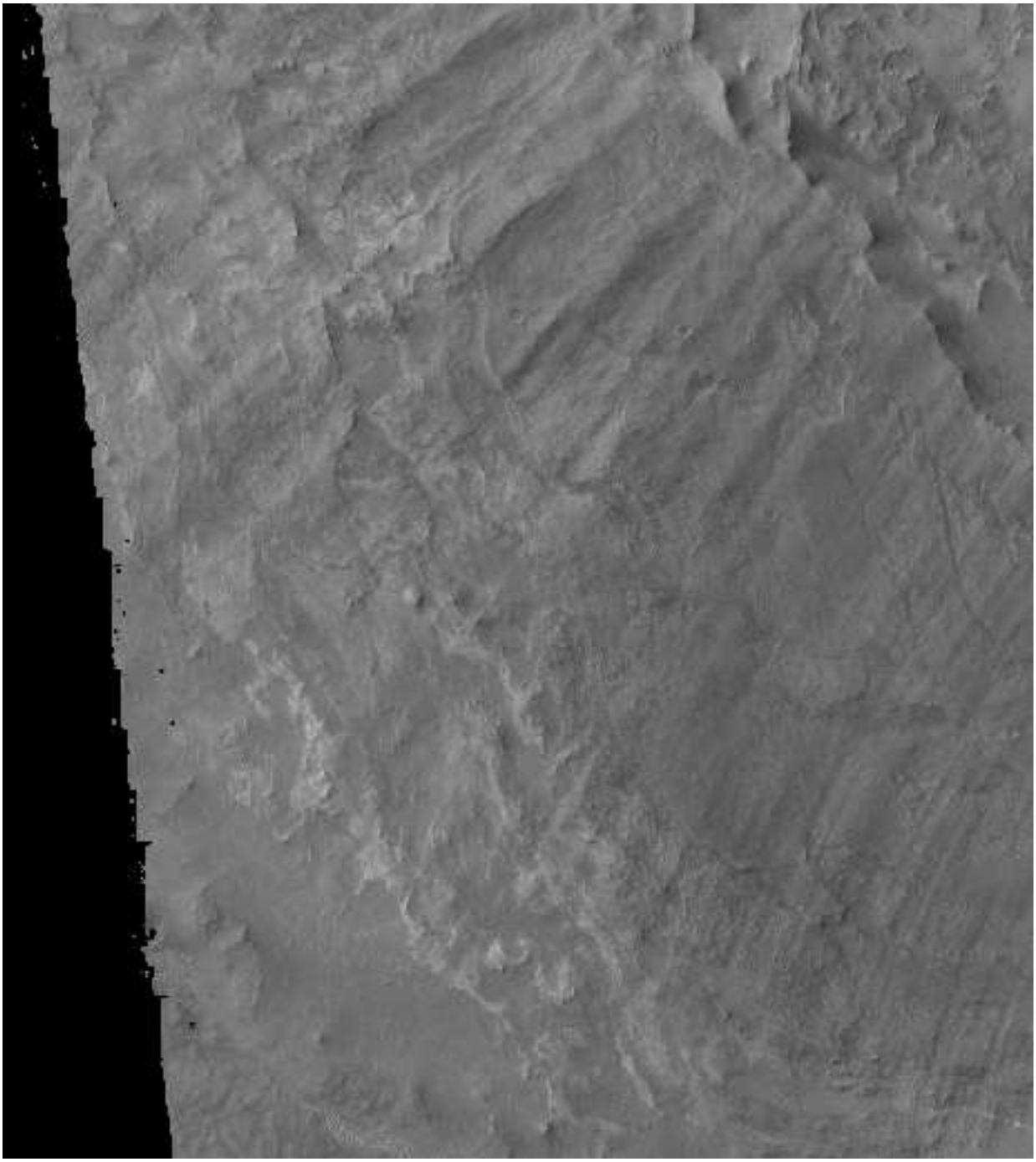

(D) Portion of CTX DTM expressing the topographic relief along the contact between units 3 and 4 visible in the HiRISE image in **2C**.

E

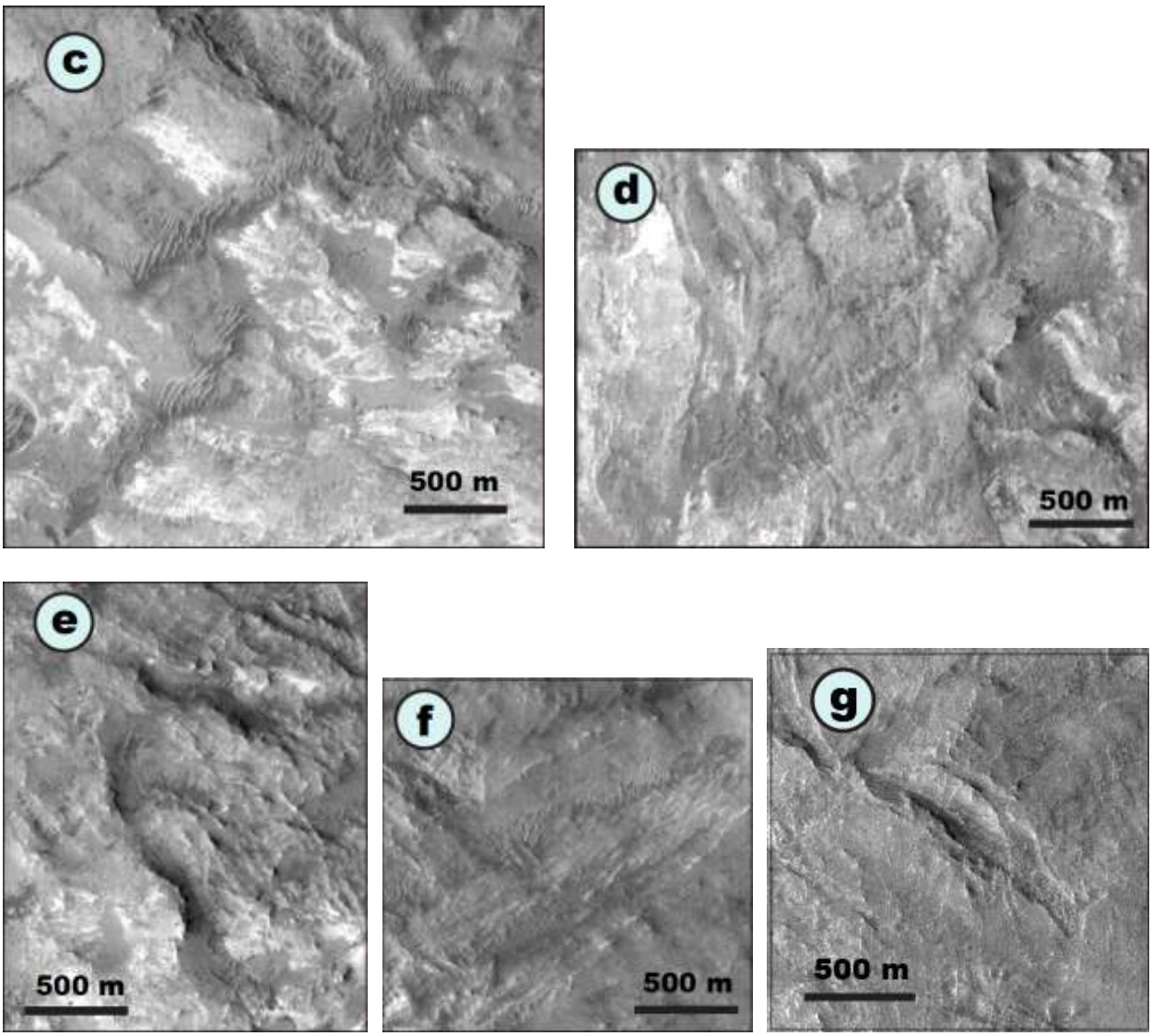


(E) Unmarked zoom-ins of features *c*, *d*, *e*, *f*, and *g* in **Fig. 2B**.

A

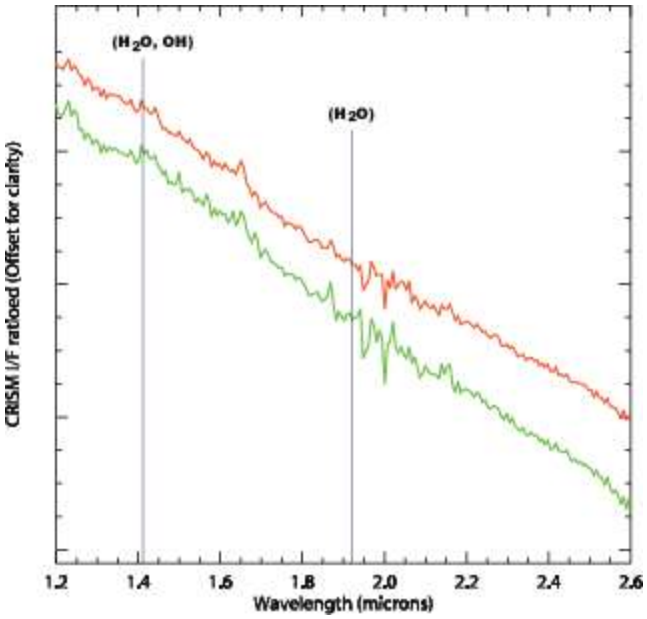
(H2O, OH)
(H2O)
CRISM I/F ratioed (Offset for clarity)
1.2
1.4
1.6
1.8
2.0
2.2
2.4
2.6
Wavelength (microns)

B

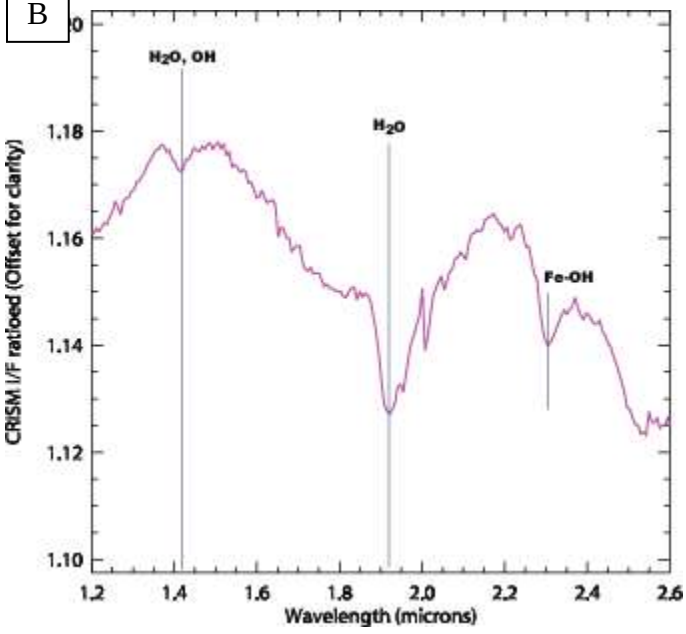
H2O, OH
H2O
Fe-OH
CRISM I/F ratioed (Offset for clarity)
1.18
1.16
1.14
1.12
1.10
1.2
1.4
1.6
1.8
2.0
2.2
2.4
2.6
Wavelength (microns)

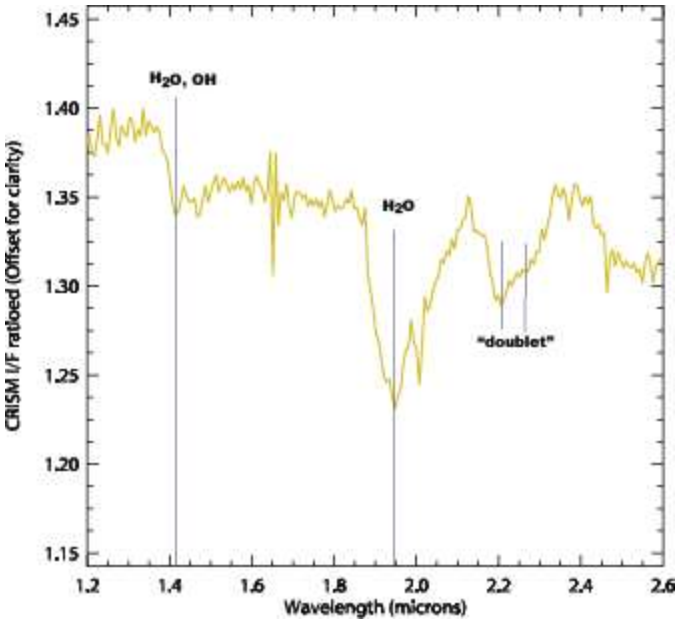


(C) Yellow-green spectra in Coprates landslide is "doublet material" (see Supp. Table 1 for pixel locations).

Supplementary Figure 3. (A) Example ratioed spectra from unhydrated portion of the landslide, CM-5, which in contrast with those in **Fig. 2**, show no absorptions related to OH or $H_2O$. (B) Additional example spectra (HRL0000A8F6) of a Coprates Chasma landslide, center lat/lon 15.187455°S/ 56.65685°W (for context see **Fig. 1**) expressing similar hydrated minerals in its debris apron to those in CM-6. Magenta spectrum is Fe/Mg smectite.